ELSEVIER

Contents lists available at ScienceDirect

# International Journal of Mass Spectrometry

journal homepage: www.elsevier.com/locate/ijms



Full Length Article

# Characterization of supramolecular peptide-polymer bioconjugates using multistage tandem mass spectrometry



Benqian Wei<sup>a</sup>, Selim Gerislioglu<sup>b</sup>, Mehmet Atakay<sup>c</sup>, Bekir Salih<sup>c</sup>, Chrys Wesdemiotis<sup>a,b,\*</sup>

- <sup>a</sup> Department of Polymer Science, The University of Akron, Akron, OH, 44325, USA
- <sup>b</sup> Department of Chemistry, The University of Akron, Akron, OH, 44325, USA
- <sup>c</sup> Department of Chemistry, Hacettepe University, 06800 Ankara, Turkey

#### ARTICLE INFO

#### Article history: Received 5 October 2018 Accepted 4 December 2018 Available online 6 December 2018

Keywords:
Non-covalent complex
Supramolecular interaction
Poly(styrene sulfonate)
Binding site analysis
ETD
ETD-CAD

## ABSTRACT

Electrospray ionization multistage tandem mass spectrometry (ESI-MS<sup>n</sup>) was employed to examine the non-covalent complexes between poly(styrene sulfonate) (PSS) and poly-L-lysine (PLL). During singlestage ion activation, the PLL peptide chain mainly underwent backbone cleavages without disruption of the non-covalent interaction which could only be broken via sequential application of electron transfer dissociation (ETD) and collisionally activated dissociation (CAD), indicating strong binding interactions between the two polyelectrolyte chains. Such binding properties make PSS a potential "non-covalent (supramolecular) label" for determining the surface accessibility of basic residues on a peptide or protein. To probe this premise, non-covalent complexes of substance P and PSS were characterized by ESI-MS<sup>n</sup> using different ion activation methods. Both MS<sup>2</sup> and MS<sup>3</sup> experiments on the substance P+PSS complex resulted in the formation of  $b_n$  (on CAD) or  $c_n$  (on ETD) fragments attached non-covalently to the intact PSS chain. All peptide fragments containing the intact PSS chain included Arg1, Lys3, and Gln5, pointing out that these residues, which are located near the N-terminus, are most likely involved in the noncovalent interaction with PSS. In contrast, Gln6 was excluded from this fragment series, attesting a much weaker interaction with PSS due to lesser accessibility. The strong tendency of PSS to bind peptides noncovalently at sites that can be elucidated by MS<sup>n</sup> demonstrates a proof-of-concept for the capacity of this approach to unveil higher order structure in proteins.

© 2018 Elsevier B.V. All rights reserved.

#### 1. Introduction

Tandem mass spectrometry (MS<sup>2</sup>) is employed extensively to investigate the non-covalent interactions in protein-protein and protein-ligand complexes [1–6]. Although the most widely mode of activation used in these studies has been collisionally activated dissociation (CAD) [5], newer MS<sup>2</sup> techniques such as electron capture dissociation (ECD) [7] and electron transfer dissociation (ETD) [8,9] have proven to be promising alternatives for the elucidation of non-covalent interactions [1,10,11]. ETD and ECD dissociate different bonds in the protein chain compared to CAD [8,12], thereby revealing complementary sequence information [13,14], without disrupting relatively weak non-covalent interactions [15,16]. Recent studies have further documented that applying ETD and CAD sequentially (MS<sup>3</sup> mode) enhances the extent of fragmentation

E-mail address: wesdemiotis@uakron.edu (C. Wesdemiotis).

vis à vis single-stage ETD or CAD [6,17–19]; this is usually performed by generating the charge-reduced precursor by ETD and subsequently activating further this ion via CAD to increase the fragmentation extent and thus gain more comprehensive structural information [20,21].

The surface of peptides and proteins is the anchoring point for binding other (bio)molecules to form multimeric complexes [22]. Consequently, it is crucial to map surface-accessible amino acid residues, as these will participate in the non-covalent interactions that ultimately lead to the multicomponent assemblies. Mass spectrometry has been the primary analytical tool for the identification of surface-accessible sites labeled by covalent chemical modification or crosslinking [22–32].

In this study, the acidic polyelectrolyte poly(styrene sulfonate) (PSS) is evaluated as a "non-covalent label", to test its suitability as a potential alternative to covalent markers for determining the basic surface-accessible residues on peptides and proteins. First, the non-covalent interactions between PSS and poly-L-lysine (PLL) were examined, since the positively charged lysine side chains are often located on the surface of hydrophilic proteins [22,31]. MS<sup>2</sup>

 $<sup>^{*}</sup>$  Corresponding author at: Department of Polymer Science, The University of Akron, Akron, OH, 44325, USA.

Fig. 1. Supramolecular PLL-PSS complex between the PLL 8-mer ( $L_8$ ) and the PSS 4-mer ( $S_4$ ). Possible hydrogen bonding interactions in [ $L_8S_4 + 2$  H]<sup>2+</sup> and the major fragment series generated by CAD ( $D_n$  and  $D_n$ ) and ETD ( $D_n$  and  $D_n$ ) are indicated in the structure.

experiments on the PLL-PSS complex showed that the non-covalent interaction between these two polyelectrolyte chains is particularly strong and can only be broken via sequential application of ETD and CAD. ETD disrupts a binding site in PLL-PSS, thereby weakening the interaction and enabling breakup of the PLL-PSS complex on subsequent CAD. The strong binding affinity of PSS for basic sites makes this polyelectrolyte a potential "non-covalent label" for determining the surface accessibility of basic residues on peptides and proteins. To probe this hypothesis, the non-covalent complexes between PSS and the peptide substance P were investigated as a proof-of-concept. As will be shown, multistage tandem mass spectrometry (MS<sup>n</sup>) involving both ETD and CAD allowed to elucidate the PSS binding location within the non-covalent (supramolecular) PSS-peptide conjugate.

# 2. Experimental

## 2.1. Chemicals

PSS sodium salt carrying the sodium sulfonate group in para position ( $M_w \approx 1100\,\text{Da}$ ) was purchased from Polymer Standards Service-USA, Inc. (Warwick, RI). Poly-L-lysine hydrobromide with an  $M_w$  range from 1000 to 5000 Da and substance P acetate salt hydrate ( $\geq 95\%$  purity) were purchased from Sigma-Aldrich (St. Louis, MO). Methanol (MeOH), ammonium acetate, and MS grade water were acquired from Fisher (Fair Lawn, NJ). All chemicals were used in the condition received without further purification.

# 2.2. MS<sup>n</sup> experiments

All experiments were performed on a Bruker HCT Ultra II quadrupole ion trap mass spectrometer equipped with an electrospray ionization (ESI) source (Bruker Daltonics, Billerica, MA). PLL and PSS solutions were prepared in 50% MeOH at the concentration of 5 µg/mL and were mixed at 1:1 (v/v) ratio to form the non-covalent complexes. For the preparation of PSS-substance P complexes, solutions of substance P and PSS were prepared in 50% MeOH that also contained 15 mM NH4OAc at the concentration of 0.01 mg/mL and 0.02 mg/mL, respectively; the latter solutions were mixed at 1:1 (v/v) ratio. All samples were injected into the ESI source using a syringe pump at a flow rate of 4 µL/min. MS² and MS³ experiments via CAD or ETD were performed on doubly and triply protonated ions. During CAD experiments, the isolation width was kept at 1.0 Da and the amplitude of the excitation

RF field was set between 0.26 and 1.10 (arbitrary units). For ETD, fluoranthene radical anions (reagent ions) were produced in a negative chemical ionization (nCI) source filled with methane buffer gas (2.0–2.6 bar) and located above the octapole lens that transfers ions from either the ESI or the nCI source to the ion trap. The reagent anion intensity was optimized at the following conditions: reagent ion ICC 100,000; ionization energy 70 eV; emission current 2.0  $\mu$ A; and reagent remove cutoff m/z 210. After accumulation of both types of species in the ion trap, the ion/ion reaction time was set within 160–170 ms. The reaction time was optimized during the MS<sup>2</sup> experiments to maximize the fragment ion abundances for the next fragmentation stage. MS and MS<sup>n</sup> data were analyzed using Bruker's Compass DataAnalysis v.4.0 software.

#### 3. Results and discussion

# 3.1. PLL-PSS complexes

The ESI-MS spectrum of solutions containing PLL ( $H-L_n-OH$ ) and PSS ( $C_4H_9-S_n-H$ ) includes doubly and triply protonated distributions of supramolecular (i.e. non-covalently bound) PLL-PSS complexes with the composition [ $L_nS_m + 2H$ ]<sup>2+</sup> and [ $L_nS_m + 3H$ ]<sup>3+</sup>, respectively (cf. Supplementary Material, Fig. S1). This notation specifies the content in repeat units of PLL ( $L_nC_6H_{12}N_2O_7$ ; 128.09 Da) and PSS ( $L_nS_m + 2H_nS_m + 2H_$ 

The MS<sup>2</sup> fragmentation patterns of doubly and triply protonated  $L_nS_m$  complexes in various stoichiometries are very similar, both upon CAD (cf. Figs. 2a vs. S2) as well as ETD (cf. Figs. 2b vs. S3). Therefore, only the MS<sup>2</sup> and MS<sup>3</sup> characteristics of triply protonated  $L_8S_4$  complex ions, viz.  $[L_8S_4 + 3\,H]^{3+}$ , will be discussed here.

CAD of  $[L_8S_4 + 3H]^{3+}$  causes amide bond cleavages in the PLL backbone, which produce homologous series of  $b_n$  and  $y_n$  fragments (Fig. 2a). Consecutive elimination of water or ammonia from the  $b_n$  fragments also takes place [33,34]. The  $b_n$  and  $y_n$  fragment series are observed both with  $(b_n^*, y_n^*)$  as well as without  $(b_n, y_n)$  the PSS chain. No peaks corresponding to the intact PLL or PSS are present in the spectrum, indicating that the non-covalent interaction between the PLL and PSS polyelectrolyte chains is stronger than the energy required for C—N bond cleavages at the PLL amide bonds.

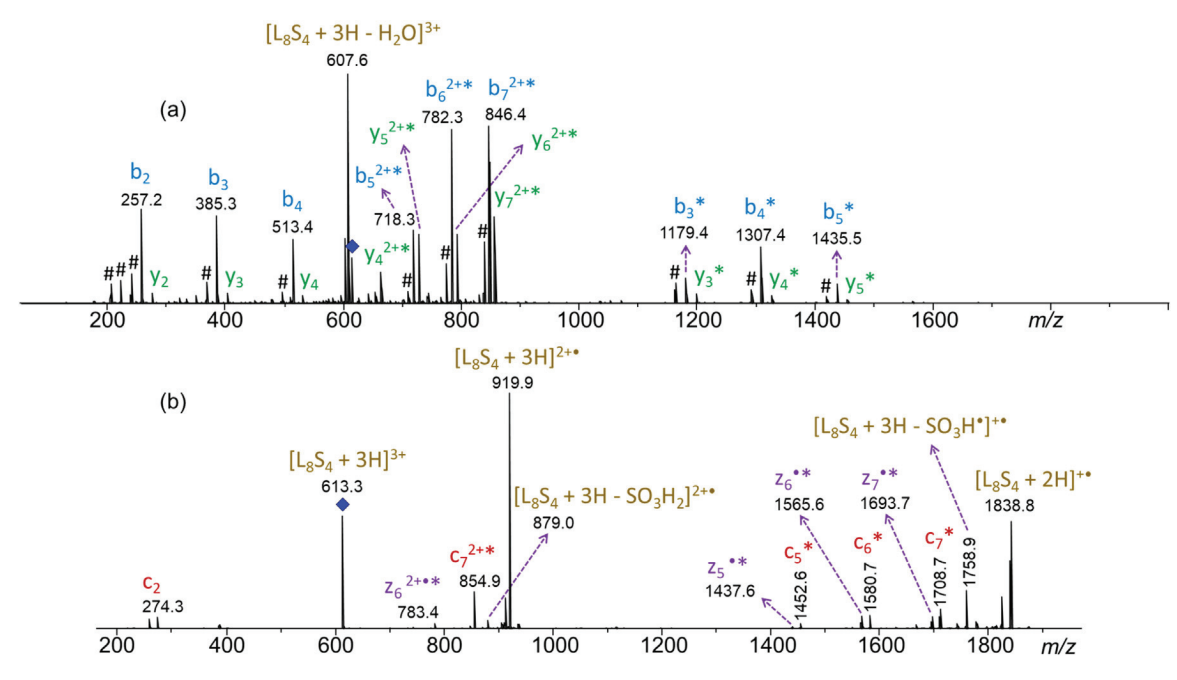


Fig. 2. (a) MS<sup>2</sup> (CAD) and (b) MS<sup>2</sup> (ETD) spectra of [ $L_8S_4 + 3H$ ]<sup>3+</sup> (m/z 613.3). A superscripted asterisk (\*) indicates fragments that contain the entire PSS chain, bound non–covalently. The sign # denotes consecutive  $H_2O$  or  $NH_3$  losses from  $b_n$  or  $b_n$ \* fragments.

The  $b_n$  and  $y_n$  fragments that do not contain the PSS chain are attributed to fragmentation of the doubly protonated PLL-PSS complex by charge separation [33,34] which generates two charged fragments, one bound to PSS non-covalently and the other without the PSS.

Under the low-energy CAD conditions used in this study, multiple collisions occur before fragmentation. The internal energy deposited in each collision is redistributed throughout the whole molecule, until enough internal energy has been accumulated to induce fragmentation within the time spent in the collision cell [35]. This slow increase of internal energy ("slow heating") promotes dissociations with low energy requirements and mainly cleaves labile bonds [19,36]. The major CAD pathways of PLL-PSS involve cleavages of the relatively weak amide bonds [37] without disruption of the supramolecular complex (Fig. 2a), corroborating the presence of strong non-covalent binding interactions between the PLL and PSS chains.

ETD experiments yield similar results with CAD, as again no dissociation of the supramolecular bioconjugate is observed to form intact PLL or PSS fragments (Fig. 2b). ETD of [L<sub>8</sub>S<sub>4</sub> + 3 H]<sup>3+</sup> primarily induces N-C<sup> $\alpha$ </sup> bond cleavages in the PLL component [7,8], generating c<sub>n</sub>\* and z<sub>n</sub>\* fragments that are bound to the intact PSS chain (cf. Fig. 2b). A unique fragmentation taking place in ETD is the elimination of a sulfonic acid radical (SO<sub>3</sub>H•, 81 Da) from the PSS side chain (Figs. 2b and S3). This dissociation is rationalized in Scheme 1 via electron transfer to a protonated lysine side chain that is hydrogenbonded with a PSS side chain. The nascent H• radical created in this step is captured by the sulfonic acid substituent, initiating the loss of SO<sub>3</sub>H•.

In contrast to CAD, unbound  $c_n$  or  $z_n$  fragments have much lower relative abundance in ETD, where the dissociating ions are mainly singly charged; when these ions undergo N–C $^{\alpha}$  bond scission, the larger fragments (i.e. those containing PSS) more effectively compete for the charge and, thus predominate. Overall, single-stage CAD or ETD do not break the non-covalent complex, verifying that the PLL and PSS polyelectrolyte chains develop strong intermolecular binding interactions.

Two ETD products, viz. the radical ion  $[L_8S_4 + 3H - SO_3H^{\bullet}]^{+\bullet}$  and the closed-shell ion  $c_7^*$ , were examined by CAD for further

information on the structure and stability of the PLL-PSS complex. Sequential ETD-CAD application (MS<sup>3</sup>) leads to a completely different outcome compared with the MS<sup>2</sup> experiments (cf. Figs. 3 vs. 2). CAD of  $[L_8S_4 + 3H - SO_3H^{\bullet}]^{+\bullet}$  results in C-N bond scissions at the PLL chain, yielding  $b_n^{\ddagger}$  and  $y_n^{\ddagger}$  fragments attached non-covalently to PSS that lost a  $-SO_3H$  side chain as well as  $b_n$  and  $y_n$  fragments devoid of PSS. It is notable that the most abundant fragment in the MS<sup>3</sup> (ETD-CAD) spectrum is the intact PLL chain (m/z 1043.7); hence, the non-covalent interaction is broken readily after the loss of SO<sub>3</sub>H<sup>•</sup>, which reduces the number of binding sites between the two polyelectrolytes. Furthermore, C-C bond scission in the PSS backbone also occurs, with concomitant dehydration, giving rise to the loss of the PSS end group ( $C_4H_{10}$ , 58 Da) plus water. This latter reaction strongly suggests that the unpaired electron in  $[L_8S_4 + 3H$ - SO<sub>3</sub>H•]<sup>+</sup>• resides on the PSS segment, from where it can initiate charge-remote homolytic bond cleavages [38] that detach the PSS end group [39].

MS³ (ETD-CAD) experiments on  $c_7^*$  also generate multiple fragment series by amide bond cleavages in the PLL backbone (Fig. 3b), which are observed either with  $(b_n^*$  and  $c_7y_n^*)$  or without  $(b_n$  and  $c_7y_n)$  the intact PSS chain attached. In addition, the non-covalent PLL-PSS interaction is broken to form the unbound  $c_7$  ion; however, the relative abundance of the latter fragment is significantly lower than the relative abundance of PSS-free [ $L_8S_4 + 3H - SO_3H^{\bullet}$ ] $^{+\bullet}$  (cf.  $c_7$  in Fig. 3b vs. [ $L_8 + H$ ] $^+$  in Fig. 3a). Evidently, the loss of one SO<sub>3</sub>H $^{\bullet}$  moiety from the PSS chain weakens markedly more the supramolecular PLL-PSS interaction than the loss of one lysine residue from the PLL chain. This phenomenon could be a consequence of the larger number of PLL vs. PSS residues in  $L_8S_4$ , which would allow PSS to find a new PLL side chain for non-covalent interaction if one lysine residue is removed.

Our MS<sup>2</sup> and MS<sup>3</sup> findings clearly indicate that the non-covalent interactions between PLL and PSS are sufficiently strong to persist after a single CAD or ETD activation event and are only disrupted by sequential ETD-CAD application. It is therefore theorized that PSS could potentially be an efficient and suitable "non-covalent label" for identifying basic surface-accessible sites of peptides and proteins by characterizing the sequence motif involved in their non-covalent interaction with PSS. This premise is evaluated here

**Scheme 1.** Elimination of a  $SO_3H^{\bullet}$  (81 Da) radical upon ETD of  $[L_8S_4 + 3H]^{3+}$  (m/z 613.3).

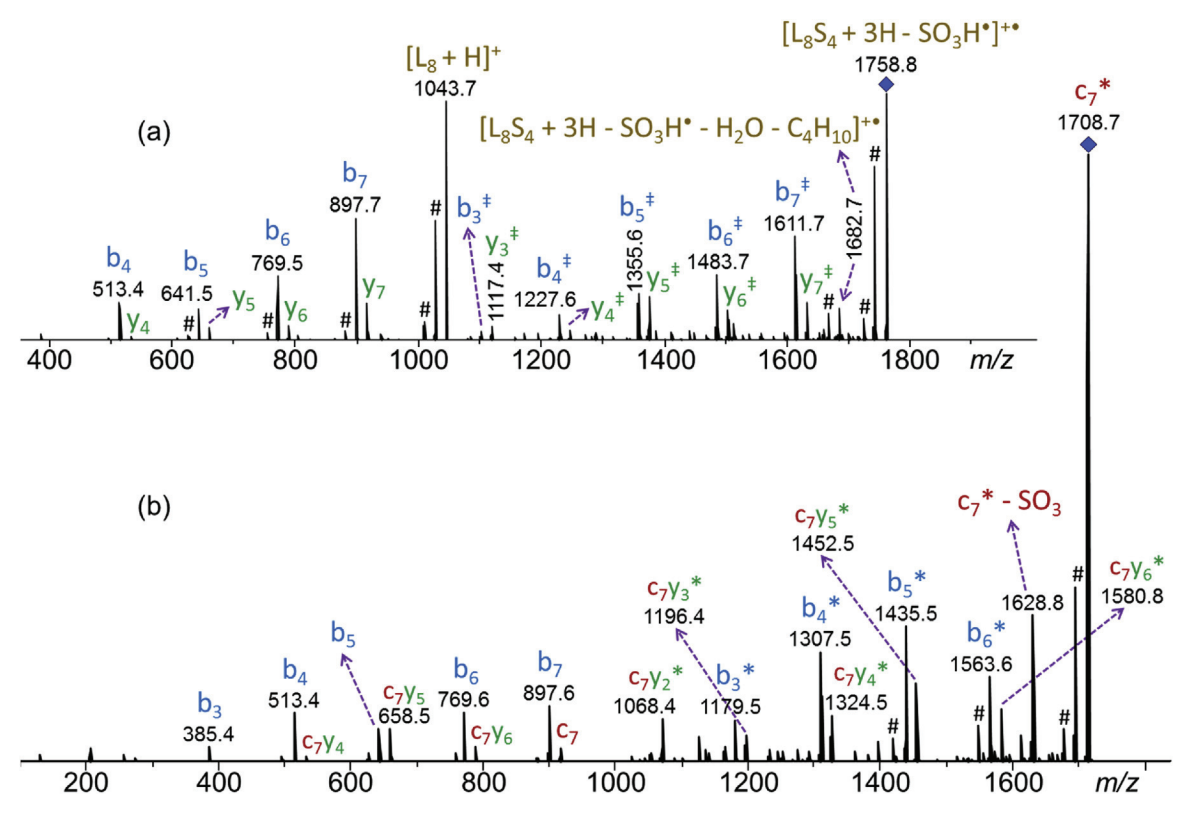


**Fig. 3.** (a) MS<sup>3</sup> (ETD-CAD) spectra of (a)  $[L_8S_4 + 3H - SO_3H^{\bullet}]^{+\bullet}$  (m/z 1758.8) and (b)  $c_7^*$  (m/z 1708.7), both generated by ETD of  $[L_8S_4 + 3H]^{3+}$  (m/z 613.3), cf. Fig. 2b. Superscripted \* or  $^{\ddagger}$  indicate fragments bound non-covalently to the intact PSS chain (\*) or a PSS chain that lost  $SO_3H^{\bullet}$  ( $^{\ddagger}$ ), respectively; the latter fragments have the compositions  $[b_nS_4 + H - SO_3H^{\bullet}]^{+}$  and  $[y_nS_4 + H - SO_3H^{\bullet}]^{+}$ . The sign # denotes consecutive  $H_2O$  or  $NH_3$  losses.

with an MS<sup>2</sup> and MS<sup>3</sup> investigation of the non-covalent complex between PSS and substance P.

# 3.2. Substance P-PSS complexes

The ESI-MS spectrum acquired from solutions containing the undecapeptide substance P (R-P-K-P-Q-Q-F-F-G-L-M) and PSS shows a series of doubly protonated supramolecular complexes with the composition  $PS_n$  (n = 3-6), where P designates substance P and  $S_n$  the non-covalently bound PSS chain, cf. Fig. S4. The most abundant complex ion, viz.  $[PS_4 + 2H]^{2+}$  (m/z 1071.9) with four PSS repeat units, was selected for MS<sup>2</sup> and MS<sup>3</sup> analysis.

CAD of  $[PS_4 + 2H]^{2+}$  induces dissociations that are diagnostic for both the strength as well as binding sites of the non-covalent interaction between substance P and PSS (Fig. 4a). A partially contiguous series of  $b_n^*$  fragments (n = 5-10) with the intact PSS chain

is observed in the CAD spectrum, along with an abundant ion corresponding to substance P minus ammonia (m/z 665.8). The latter fragment provides compelling evidence that the non-covalent interaction between substance P and PSS is considerably weaker than that holding the PLL-PSS complex together. This observation is attributed to the presence of fewer potential binding sites on substance P whose sequence contains several amino acid residues with lower basicity compared to lysine.

In contrast to the CAD fragmentation pattern of substance P itself, which includes the formation of small  $a_n$  and  $b_n$  fragments (n = 2-3, cf. Fig. S5a), the smallest  $b_n$ \* fragment generated by CAD of the supramolecular bioconjugate is  $b_5$ \* (cf. Fig. 4a). This fragment contains the likely PSS binding sites Arg1, Lys3, and Gln5 which are located near the N-terminus, but not Gln6, which is another basic and, hence, potential binding site for an acidic polyelectrolyte. Our results strongly suggest that the former three amino acid residues

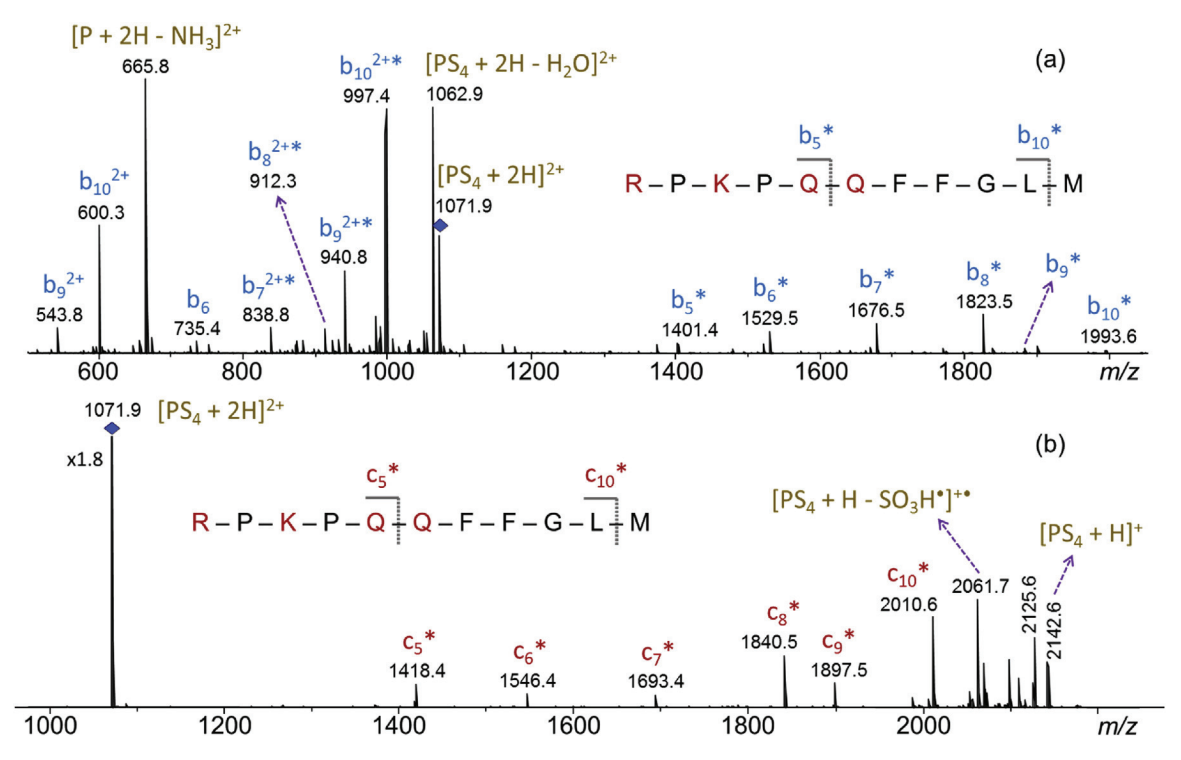


**Fig. 4.** (a) MS<sup>2</sup> (CAD) and (b) MS<sup>2</sup> (ETD) spectra of [PS<sub>4</sub> + 2 H]<sup>2+</sup> (m/z 1071.9). A superscripted asterisk (\*) indicates fragments that contain the entire PSS chain, bound non–covalently. Fragments  $c_n^*$  - 1 and [PS<sub>4</sub> + H - SO<sub>3</sub>H<sub>2</sub>]<sup>+</sup> are also present in the ETD spectrum.

are involved in the non-covalent interaction, whereas Gln6 is not, or is much more weakly involved in such an interaction, presumably because its side chain extends in the opposite direction relative to those of Arg1, Lys3, and Gln5 in the substance P conformer sampled in the bioconjugation medium (see Experimental, section 2.2) [40]. Further validation of this assumption was sought by ETD and MS³ experiments.

ETD of  $[PS_4 + 2H]^{2+}$  yields a contiguous series of  $c_n^*$  fragments down to  $c_5^*$ , in striking similarity to CAD which yielded a continuous series of  $b_n^*$  fragments down to  $b_5^*$  (Fig. 4b vs. a). Under ETD conditions, however, the non-covalent interaction between substance P and PSS is not broken, as no ions characteristic of detached substance P are observed. This difference between ETD and CAD is accounted for by the non-ergodic feature of the ETD process, which preserves the relatively labile non-covalent interaction between the undecapeptide and PSS [7,8].

Compared to ETD of substance P, which causes fragmentation of essentially all N–C $^{\alpha}$  bonds to form almost complete  $c_n$  and  $z_n$ • fragment series (Fig. S5), ETD of the PSS conjugate of this undecapeptide only produces the N-terminal  $c_n$ \* series comprising the intact PSS chain (Fig. 4b), with the smallest fragment having five residues ( $c_5$ \*), in full agreement with the CAD results. This observation confirms that Gln6 may not be involved in the non-covalent interaction between substance P and PSS, while the other three basic residues (Arg1, Lys3, and Gln5), which are closer to the N-terminus, are more likely to be the binding sites. Lastly, it is worth noting that a fragment arising by elimination of a SO<sub>3</sub>H• radical from PSS is also present in the ETD spectrum (Fig. 4b); as discussed earlier, such a fragment corroborates the existence of non-covalent binding between a basic amino acid side chain and a –SO<sub>3</sub>H pendant on PSS (vide supra and Scheme 1).

Sequential ETD-CAD was applied to  $c_{10}^*$  ions to verify the conclusions drawn from the single-stage ETD and CAD experiments. As expected, this fragment which represents the PSS conjugate of a truncated substance P (C-terminal Met is missing), and the original bioconjugate of intact substance P give rise to very similar CAD

spectra, both showing a  $b_n^*$  fragment series down to  $b_5^*$ , cf. Figs. 5 vs. 4a. Furthermore, the non-covalent interaction between  $c_{10}$  and PSS is cleaved (Fig. 5), as also observed for the bioconjugate between intact substance P and PSS (Fig. 4a); this reconciles the presence of unbound  $b_n$  and internal  $c_{10}y_n$  fragments in the MS<sup>3</sup> spectrum (Fig. 5).

Overall, both the MS<sup>2</sup> and MS<sup>3</sup> data validate that Gln6 plays a minor role in the non-covalent interaction with PSS, as compared to Arg1, Lys3, and Gln5. This in turn indicates that Arg1, Lys3 and Gln5 must be the surface-accessible basic sites of substance P that sense an approaching anionic polyelectrolyte like PSS, as also suggested by published NMR data [40].

#### 4. Conclusions

MS<sup>2</sup> experiments on supramolecular PLL-PSS complexes, via either CAD or ETD, cause predominantly bond cleavages in the PLL backbone without disruption of the non-covalent interaction between PLL and PSS, which can only be broken by consecutive fragmentation via CAD of select ETD products. The ability to sequence peptide chains without affecting their non-covalent intermolecular binding to PSS reveals that PSS could act as an effectual "label" for determining the surface accessibility of basic residues on peptides or proteins by identification of the sequence motif containing the PSS label.

This premise was evaluated by elucidating the binding site of PSS in its supramolecular complex with substance P. Peptide fragments with the PSS chain were observed down to  $b_5^*$  (by CAD) or  $c_5^*$  (by ETD), indicating that amino acids up to residue 5 must be involved in the non-covalent binding of PSS and that Gln6 is not involved in the non-covalent interaction and, hence, is not an exposed site that can develop binding interactions with PSS. On the other hand, the participation of Arg1, Lys3, and Gln5 in the non-covalent binding of PSS is confirmed, since they are contained in all supramolecular fragments observed. Consequently, Arg1, Lys3, and Gln5 are the most likely surface-accessible sites of substance P. The

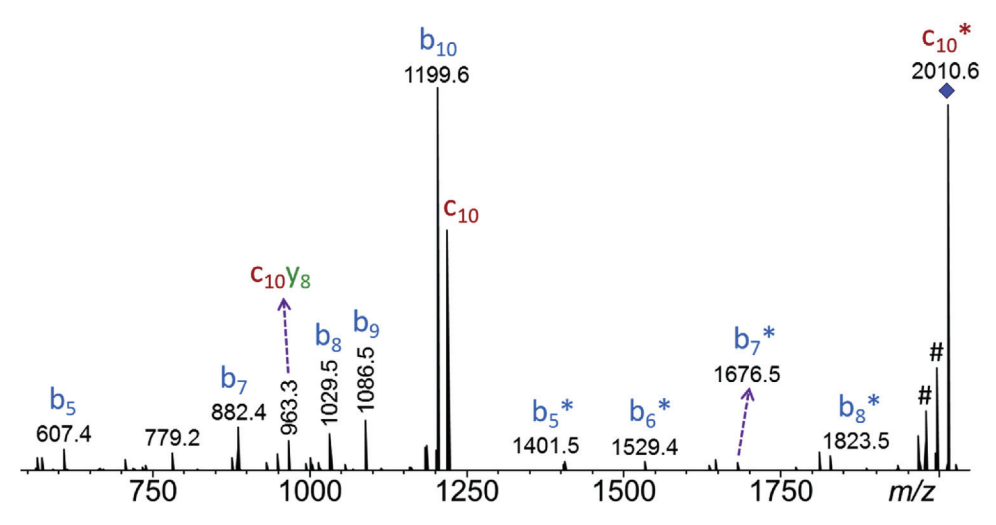


Fig. 5. MS<sup>3</sup> (ETD-CAD) spectrum of  $c_{10}^*$  (m/z 2010.6), generated by ETD of [PS<sub>4</sub> + 2 H]<sup>2+</sup> (m/z 1071.9), cf. Fig. 4b. A superscripted asterisk (\*) indicates fragments bound non–covalently to the PSS chain. The sign # denotes consecutive H<sub>2</sub>O or NH<sub>3</sub> losses.

non-covalent interaction between substance P and PSS is, however, weaker than that in the PLL-PSS complex, as it can be broken via single-stage CAD.

The results of this study present a proof-of-concept for the effectiveness of PSS as a potential "non-covalent label" for the investigation of the surface accessibility of basic residues on biomolecules. Work in progress is extending this analytical concept to proteins.

#### Acknowledgements

We thank the National Science Foundation for generous financial support (CHE-1808115). M. Atakay acknowledges The Scientific and Technological Research Council of Turkey (TUBITAK) for supporting part of his PhD studies at The University of Akron through Program 2214-A.

# Appendix A. Supplementary data

Supplementary material related to this article can be found, in the online version, at doi:https://doi.org/10.1016/j.ijms.2018.12.005.

#### References

- [1] S. Yin, J.A. Loo, Elucidating the site of protein-ATP binding by top-down mass spectrometry, J. Am. Soc. Mass Spectrom. 21 (2010) 899–907, http://dx.doi. org/10.1016/j.jasms.2010.01.002.
- [2] D.J. Clarke, E. Murray, T. Hupp, C.L. MacKay, P.R.R. Langridge-Smith, Mapping a noncovalent protein-peptide interface by top-down FTICR mass spectrometry using electron capture dissociation, J. Am. Soc. Mass Spectrom. 22 (2011) 1432–1440, http://dx.doi.org/10.1007/s13361-011-0155-3.
- [3] N.P. Barrera, C.V. Robinson, Advances in the mass spectrometry of membrane proteins: from individual proteins to intact complexes, Annu. Rev. Biochem. 80 (2011) 247–271, http://dx.doi.org/10.1146/annurev-biochem-062309-023237
- [4] J.P. O'Brien, W. Li, Y. Zhang, J.S. Brodbelt, Characterization of native protein complexes using ultraviolet photodissociation mass spectrometry, J. Am. Chem. Soc. 136 (2014) 12920–12928, http://dx.doi.org/10.1021/ja505217w.
- [5] F. Chen, B. Gülbakan, S. Weidmann, S.R. Fagerer, A.J. Ibáñez, R. Zenobi, Applying mass spectrometry to study non-covalent biomolecule complexes, Mass Spectrom. Rev. 35 (2016) 48–70, http://dx.doi.org/10.1002/mas.21462.
- [6] H.H. Nguyen, R.R. Ogorzalek Loo, I.D.G. Campuzano, J.A. Loo, An integrated native mass spectrometry and top-down proteomics method that cannects sequence to structure and function of macromolecular complexes, Nat. Chem. 10 (2018) 139–148, http://dx.doi.org/10.1038/nchem.2908.
- [7] R. Zubarev, N.L. Kelleher, F.W. McLafferty, Electron capture dissociation of multiply charged protein cations, A nonergodic process, J. Am. Chem. Soc. 120 (1998) 3265–3266, http://dx.doi.org/10.1021/ja973478k.

- [8] J.E.P. Syka, J.J. Coon, M.J. Schroeder, J. Shabanowitz, D.F. Hunt, Peptide and protein sequence analysis by electron transfer dissociation mass spectrometry, Proc. Natl. Acad. Sci. U. S. A. 101 (2004) 9528–9533, http://dx. doi.org/10.1073/pnas.0402700101.
- [9] S.J. Pitteri, S.A. McLuckey, Recent developments in the ion/ion chemistry of high-mass multiply charged ions, Mass Spectrom. Rev. 24 (2005) 931–958, http://dx.doi.org/10.1002/mas.20048.
- [10] L. Sleno, D.A. Volmer, Ion activation methods for tandem mass spectrometry, J. Mass Spectrom. 39 (2004) 1091–1112, http://dx.doi.org/10.1002/jms.703.
- [11] Y. Xie, J. Zhang, S. Yin, J.A. Loo, Top-down ESI-ECD-FT-ICR mass spectrometry localizes noncovalent protein-ligand binding sites, J. Am. Chem. Soc. 128 (2006) 14432–14433, http://dx.doi.org/10.1021/ja063197p.
- [12] K.O. Zhurov, L. Fornelli, M.D. Wodrich, Ü.A. Laskay, Y.O. Tsybin, Principles of electron capture and transfer dissociation mass spectrometry applied to peptide and protein structure analysis, Chem. Soc. Rev. 42 (2013) 5014–5030, http://dx.doi.org/10.1039/c3cs35477f.
- [13] J.J. Coon, Collision or electron? Protein sequence analysis on the 21st century, Anal. Chem. 81 (2009) 3208–3215, http://dx.doi.org/10.1021/ac802330b.
- [14] N.M. Riley, J.J. Coon, The role of electron transfer dissociation in modern proteomics, Anal. Chem. 90 (2018) 40–64, http://dx.doi.org/10.1021/acs. analchem.7b04810.
- [15] K.F. Haselmann, T.J.D. Jørgensen, B.A. Budnik, F. Jensen, R.A. Zubarev, Electron capture dissociation of weakly bound polypeptide polycationic complexes, Rapid Commun. Mass Spectrom. 16 (2002) 2260–2265, http://dx.doi.org/10. 1002/rcm.853.
- [16] S. Yin, J.A. Loo, Top-down mass spectrometry of supercharged native protein-ligand complexes, Int. J. Mass Spectrom. 300 (2011) 118–122, http:// dx.doi.org/10.1016/j.ijms.2010.06.032.
- [17] D.L. Swaney, G.C. McAlister, M. Wirtala, J.C. Schwartz, J.E.P. Syka, J.J. Coon, Supplemental activation method for high-efficiency electron-transfer dissociation of doubly protonated peptide precursors, Anal. Chem. 79 (2007) 477–485, http://dx.doi.org/10.1021/ac061457f.
- [18] Z. Zhang, S.J. Browne, R.W. Vachet, Exploring salt bridge structures of gas-phase protein ions using multiple stages of electron transfer and collision induced dissociation, J. Am. Soc. Mass Spectrom. 25 (2014) 604–613, http:// dx.doi.org/10.1007/s13361-013-0821-8.
- [19] S. Gerislioglu, C. Wesdemiotis, Chain-end and backbone analysis of poly(N-isopropylacrylamide)s using sequential electron transfer dissociation and collisionally activated dissociation, Int. J. Mass Spectrom. 413 (2017) 61–68, http://dx.doi.org/10.1016/j.ijms.2016.08.001.
- [20] Y. Gao, S.A. McLuckey, Electron transfer followed by collision-induced dissociation (NET-CID) for generating sequence information from backbone modified oligonucleotide anions, Rapid Commun. Mass Spectrom. 27 (2013) 249–257, http://dx.doi.org/10.1002/rcm.6428.
- [21] B.C. Katzenmeyer, L.R. Cool, J.P. Williams, K. Craven, J.M. Brown, C. Wesdemiotis, Electron transfer dissociation of sodium cationized polyesters: reaction time effects and combination with collisional activation and ion mobility separation, Int. J. Mass Spectrom. 378 (2015) 303–311, http://dx.doi.org/10.1016/j.ijms.2014.09.021.
- [22] L. Vasicek, J.P. O'Brien, K.S. Browning, Z. Tao, H.-W. Liu, J.S. Brodbelt, Mapping protein surface accessibility via an electron transfer dissociation selectively cleavable hydrazone probe, Mol. Cell. Proteomics 11 (2012), http://dx.doi.org/ 10.1074/mcp.0111.015826, 0111.015826-0111.015826.
- [23] D. Suckau, M. Mak, M. Przybylski, Protein surface topology-probing by selective chemical modification and mass spectrometric peptide mapping, Proc. Natl. Acad. Sci. U. S. A. 89 (1992) 5630–5634, http://dx.doi.org/10.1073/ pnas.89.12.5630.

- [24] M.O. Glocker, C. Borchers, W. Fiedler, D. Suckau, M. Przybylski, Molecular characterization of surface topology in protein tertiary structures by amino-acylation and mass spectrometric peptide mapping, Bioconjug. Chem. 5 (1994) 583–590, http://dx.doi.org/10.1021/bc00030a014.
- [25] F. Zappacosta, P. Ingallinella, A. Scaloni, A. Pessi, E. Bianchi, M. Sollazzo, A. Tramontano, G. Marino, P. Pucci, Surface topology of Minibody by selective chemical modifications and mass spectrometry, Protein Sci. 6 (1997) 1901–1909, http://dx.doi.org/10.1002/pro.5560060911.
- [26] B. Salih, R. Zenobi, MALDI mass spectrometry of dye-peptide and dye-protein complexes, Anal. Chem. 70 (1998) 1536–1543, http://dx.doi.org/10.1021/ ac9708506.
- [27] B.T. Turner Jr., T.M. Sabo, D. Wilding, M.C. Maurer, Mapping of factor XIII solvent accessibility as a function of activation state using chemical modification methods, Biochemistry 43 (2004) 9755–9765, http://dx.doi.org/ 10.1021/bi049260+.
- [28] A. Leitner, W. Lindner, Functional probing of arginine residues in proteins using mass spectrometry and an arginine-specific covalent tagging concept, Anal. Chem. 77 (2005) 4481–4488, http://dx.doi.org/10.1021/ac050217h.
- [29] A. Scholten, N.F.C. Visser, R.H.H. van den Heuvel, A.J.R. Heck, Analysis of protein-protein interaction surfaces using a combination of efficient lysine acetylation and nanoLC-MALDI-MS/MS applied to the E9:Im9 bacteriotoxin-immunity protein complex, J. Am. Soc. Mass Spectrom. 17 (2006) 983–994, http://dx.doi.org/10.1016/j.jasms.2006.03.005.
- [30] V.L. Mendoza, R.W. Vachet, Protein surface mapping using diethylpyrocarbonate with mass spectrometric detection, Anal. Chem. 80 (2008) 2895–2904, http://dx.doi.org/10.1021/ac701999b.
- [31] V.L. Mendoza, R.W. Vachet, Probing protein structure by amino acid-specific covalent labeling and mass spectrometry, Mass Spectrom. Rev. 28 (2009) 785–815, http://dx.doi.org/10.1002/mas.20203.
- [32] T. Liu, T.M. Marcinko, P.A. Kiefer, R.W. Vachet, Using covalent labeling and mass spectrometry to study protein binding sites of amyloid inhibiting

- molecules, Anal. Chem. 89 (2017) 11583–11591, http://dx.doi.org/10.1021/acs.analchem.7b02915.
- [33] X.-J. Tang, R.K. Boyd, An investigation of fragmentation mechanisms of doubly protonated tryptic peptides, Rapid Commun. Mass Spectrom. 6 (1992) 651–657, http://dx.doi.org/10.1002/rcm.1290061105.
- [34] P. Wang, M.M. Kish, C. Wesdemiotis, Fragmentation mechanisms of peptide ions, in: R.S. Caprioli, M.L. Gross (Eds.), The Encyclopedia of Mass Spectrometry, Part A, vol. 2, Elsevier, Amsterdam, 2005, pp. 139–151, ISBN: 0080438008.
- [35] V. Scionti, C. Wesdemiotis, Tandem mass spectrometry analysis of polymer structures and architectures, in: C. Barner-Kowollik, in: T. Gruendling, J. Falkenhagen, S. Weidner (Eds.), Mass Spectrometry in Polymer Chemistry, Wiley-VCH, Weinheim, 2012, pp. 57–84, http://dx.doi.org/10.1002/ 9783527641826. ch3.
- [36] C. Wesdemiotis, N. Solak, M.J. Polce, D.E. Dabney, K. Chaicharoen, B.C. Katzenmeyer, Fragmentation pathways of polymer ions, Mass Spectrom. Rev. 30 (2011) 523–529, http://dx.doi.org/10.1002/mas.20282.
- [37] J. Laskin, Surface-induced dissociation: a unique tool for studying energetics and kinetics of the gas-phase fragmentation of large ions, Eur. J. Mass Spectrom. 21 (2015) 377–389, http://dx.doi.org/10.1255/ejms.1358.
- [38] C. Cheng, M.L. Gross, Applications and mechanisms of charge-remote fragmentation, Mass Spectrom. Rev. 19 (2000) 398–420, http://dx.doi.org/10. 1002/1098-2787(2000)19:6<398, :AID-MAS3>3.0.CO;2-B.
- [39] M.J. Polce, M. Ocampo, R.P. Quirk, A.M. Leigh, C. Wesdemiotis, Tandem mass spectrometry characteristics of silver-cationized polystyrenes: internal energy, size, and chain end versus backbone substituent effects, Anal. Chem. 80 (2008) 355–362, http://dx.doi.org/10.1021/ac701917x.
- [40] G. Chassaing, O. Convert, S. Lavielle, Preferential conformation of substance P in solution, Eur. J. Biochem. 154 (1986) 77–85, http://dx.doi.org/10.1111/j. 1432-1033.1986.tb09361.x.